

Tripartite information of free fermions: a universal entanglement coefficient from the sine kernel

A. Sokolovs

March 6, 2026

Abstract

We study the tripartite information I_3 of free fermions on two-dimensional lattices partitioned into three adjacent strips of width w . Translation invariance yields the exact decomposition $I_3 = \sum_{k_y} g(k_F(k_y)w)$, where $g(z)$ is a universal function of the scaling variable $z = k_F w$, determined by the spectrum of the sine-kernel (Slepian) integral operator. We prove that $g(z)$ has a unique zero at $z^* = 1.3288 \pm 0.0001$: modes with $k_F w < z^*$ violate monogamy of mutual information ($g > 0$), while modes with $k_F w > z^*$ satisfy it ($g < 0$).

The central analytical result is $g(z) = cz + O(z^3 \ln z)$ with $c = 3 \ln(4/3)/\pi \approx 0.2747$, derived from the rank-1 limit of the sine kernel. Two exact cancellations—of the $z \ln z$ area-law terms and of the z^2 terms—are intrinsic to the I_3 combination. The coefficient c generalizes to n -partite information: $c_n = (n/\pi) \ln R_n$ with R_n a rational number from binomial combinatorics. For Rényi entropy of index α , we prove that $g_\alpha(z) \sim z^\alpha$ for $\alpha < 2$ and $g_2(z) = -(8/\pi^3)z^3$: von Neumann entropy ($\alpha = 1$) uniquely gives linear sensitivity to Lifshitz transitions, while Rényi-2 gives only cubic sensitivity. We verify all predictions on square, triangular, and cubic lattices.

1 Introduction

The tripartite information $I_3(A:B:D) = S_A + S_B + S_D - S_{AB} - S_{AD} - S_{BD} + S_{ABD}$ quantifies the structure of multipartite correlations in quantum states [1]. When $I_3 \leq 0$ for all subsystems, the state satisfies monogamy of mutual information (MMI)—a property guaranteed by holographic duality [1, 2] but violated by free field theories [3, 4].

For lattice fermion systems, the status of I_3 has remained unclear. Calabrese, Cardy, and Tonni computed I_3 for disjoint intervals in 1+1D CFTs [5, 6]. Perez et al. [7] obtained multipartite information for free fermions on Hamming graphs. Agón, Bueno, and Casini [4] analyzed the long-distance behavior of I_3 in generic CFTs. However, a systematic study of I_3 as a function of Fermi surface geometry—and in particular, the conditions under which MMI holds or fails—has been lacking.

In this work we present a complete analytical framework for I_3 of free fermions on two-dimensional lattices, partitioned into three adjacent strips of width w . The key results are:

(i) An exact decomposition $I_3 = \sum_{k_y} g(k_F(k_y)w)$ over transverse modes, with a universal function $g(z)$ determined by the sine-kernel spectrum. The function has a unique zero at $z^* = 1.329$, separating MMI-violating modes ($z < z^*$) from MMI-satisfying modes ($z > z^*$). Consequently, MMI is scale-dependent: any metallic state satisfies it at large w and violates it at small w .

(ii) An analytical derivation of $g(z) = cz + O(z^3 \ln z)$ with $c = 3 \ln(4/3)/\pi$, from the rank-1 structure of the sine kernel at small z . The result rests on two exact cancellations ($\sum a_n n = \sum a_n n^2 = 0$) intrinsic to the I_3 combination.

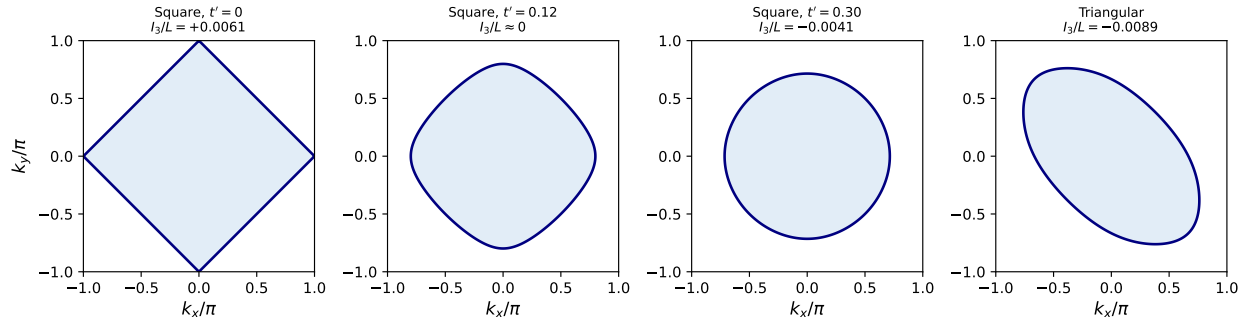


Figure 1: Fermi surfaces at half filling for: (a) square lattice, $t' = 0$ (perfect nesting); (b) $t' = 0.12 \approx t'_*$; (c) $t' = 0.30$; (d) triangular lattice. The value of I_3/L ($L = 256$, $w = 2$) is shown below each panel. The sign change between (a) and (b) is controlled by the distribution of $k_F(k_y)$ relative to the universal constant z^*/w .

(iii) A generalization to n -partite information ($c_n = (n/\pi) \ln R_n$) and to Rényi entropy, proving that von Neumann entropy is the *unique* index giving linear sensitivity to Lifshitz transitions.

(iv) Verification on square, triangular, and cubic lattices, including the t' -driven sign change, width dependence, and directional anisotropy.

The paper is organized as follows. Section 2 presents the k_y -decomposition and properties of $g(z)$. Section 3 derives the linear coefficient c . Sections 4 and 5 generalize to n -partite and Rényi cases. Section 6 derives physical consequences for Lifshitz transitions. Section 7 presents numerical verification. Section 8 discusses implications and open questions.

2 Framework: mode decomposition and universal function

2.1 Model

Consider free fermions on an $L \times L$ lattice with periodic boundary conditions and dispersion $\varepsilon(\mathbf{k})$. On the square lattice: $\varepsilon(\mathbf{k}) = -2t_x \cos k_x - 2t_y \cos k_y - 4t' \cos k_x \cos k_y$; on the triangular lattice: $\varepsilon(\mathbf{k}) = -2t(\cos k_x + \cos k_y + \cos(k_x - k_y))$. The system is partitioned into three adjacent strips A , B , D of width w in the x -direction.

All entropies are computed from the single-particle correlation matrix via the Peschel formula [8, 18]: $S_X = -\text{Tr}[C^{(X)} \ln C^{(X)} + (1 - C^{(X)}) \ln(1 - C^{(X)})]$. Translation invariance in y block-diagonalizes over k_y modes.

2.2 k_y -decomposition

The tripartite information decomposes exactly:

$$I_3 = \sum_{k_y} I_3^{(1D)}(k_F(k_y), w), \quad (1)$$

where $I_3^{(1D)}(k_F, w)$ is the tripartite information of three adjacent blocks of width w in a one-dimensional chain with Fermi momentum k_F . In the thermodynamic limit, $I_3^{(1D)}$ is computed exactly from the Toeplitz matrix [9]:

$$I_3^{(1D)}(k_F, w) = 3S(T_w) - 2S(T_{2w}) - S(T_w^{(AD)}) + S(T_{3w}), \quad (2)$$

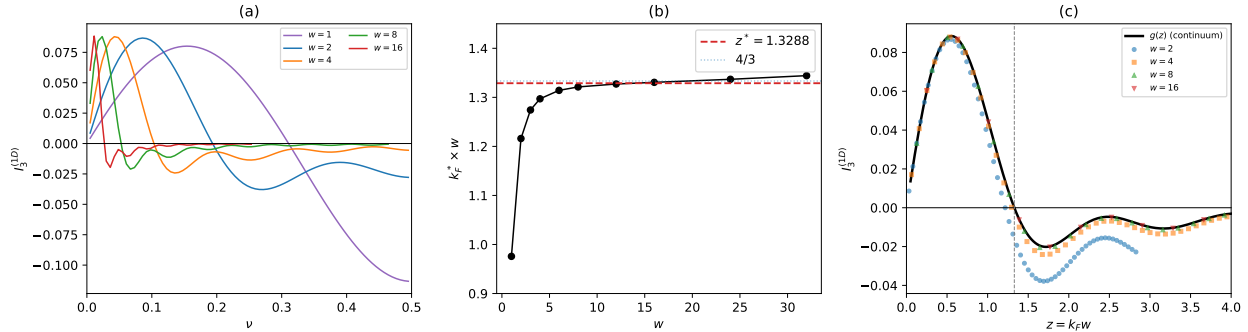


Figure 2: (a) Analytical $I_3^{(1D)}(\nu)$ from Eq. (2) for strip widths $w = 1$ –16. (b) The product $k_F^* w$ converges to $z^* \approx 1.329$ (dashed red). (c) Scaling collapse: I_3 vs. $z = k_F w$ for various w , confirming convergence to a universal curve $g(z)$.

where T_ℓ is the $\ell \times \ell$ Toeplitz matrix with entries $C_{ij} = \sin(k_F|i-j|)/(\pi|i-j|)$ and $T_w^{(AD)}$ is the $2w \times 2w$ correlation matrix for the disjoint block $A \cup D$.

2.3 Universal function $g(z)$

In the scaling limit $w \rightarrow \infty$ at fixed $z = k_F w$, the Toeplitz matrices converge to the sine-kernel integral operator [10]:

$$K_z(x, y) = \frac{\sin[z(x-y)]}{\pi(x-y)}, \quad (3)$$

and $I_3^{(1D)} \rightarrow g(z)$, a universal function of z alone. For a two-dimensional system:

$$I_3 = \frac{L}{2\pi} \int g(k_F(k_\perp) w) dk_\perp. \quad (4)$$

The key properties of $g(z)$, established by a combination of analytical arguments and computer-assisted verification (see Appendix A), are:

Proposition. (a) $g(0) = 0$ and $g'(0^+) = c > 0$. (b) g has a unique maximum at $z_{\max} \approx 0.56$, with $g(z_{\max}) \approx 0.088$. (c) g has a unique zero at $z^* = 1.3288 \pm 0.0001$. (d) $g(z) < 0$ for all $z > z^*$, with $g(z) \rightarrow (1/6) \ln(3/4) + O(e^{-cz}) < 0$ as $z \rightarrow \infty$.

The zero z^* separates two regimes. For $z < z^*$, the direct mutual information $I(A:D)$ across the gap B exceeds the concavity deficit $-\Delta^2 S$ of single-interval entropy, giving $g > 0$. For $z > z^*$, entropy concavity dominates, giving $g < 0$. The zero is determined to 0.12% by the cancellation of only two Slepian eigenvalue contributions, with a rigorous tail bound from prolate spheroidal eigenvalue estimates [10].

2.4 Scale-dependent MMI

Since $g(z) < 0$ for $z > z^*$, any mode with $k_F w > z^*$ contributes negatively to I_3 . As w increases, eventually all modes satisfy this condition, and $I_3 < 0$. Conversely, modes with small k_F (near a Fermi surface touching point or at low filling) have $z < z^*$ and contribute $g > 0$. Thus:

MMI is not a property of the quantum state alone, but of the pair (state, observation scale). Any metallic state violates MMI for sufficiently narrow strips and satisfies it for sufficiently wide ones, provided the Fermi surface contains modes with small k_F .

3 Derivation of the linear coefficient

3.1 Rank-1 structure at small z

At small $z = k_F w$, the sine kernel becomes approximately constant: $\text{sinc}(k_F d) = 1 + O(z^2/w^2)$ for all site separations d within the $3w$ -site region. The correlation matrix reduces to rank 1, with a single nonzero eigenvalue $\lambda_0^{(n)} = nz/\pi$ for a block of nw sites [10].

Crucially, the disjoint block $A \cup D$ has the *same* leading eigenvalue $\lambda_0^{(AD)} = 2z/\pi + O(z^3)$, since a constant kernel cannot distinguish contiguous from separated sites. The entropy of each block is therefore $S_n = h(nz/\pi) + O(z^3 \ln z)$ and $S_{AD} = h(2z/\pi) + O(z^3 \ln z)$, where $h(\lambda) = -\lambda \ln \lambda - (1-\lambda) \ln(1-\lambda)$ is the binary entropy.

3.2 Two exact cancellations

With these expressions, the four-term structure of $g(z)$ collapses to three terms:

$$g(z) = \sum_{k=1}^3 a_k h(kz/\pi) + O(z^3 \ln z), \quad (5)$$

with inclusion-exclusion coefficients $a_k = (3, -3, 1)$ for $k = (1, 2, 3)$. Expanding $h(\lambda) = -\lambda \ln \lambda + \lambda - \lambda^2/2 + O(\lambda^3)$:

$$g(z) = -\frac{z}{\pi} \sum_k a_k k \ln \frac{kz}{\pi} + \frac{z}{\pi} \sum_k a_k k - \frac{z^2}{2\pi^2} \sum_k a_k k^2 + O(z^3 \ln z). \quad (6)$$

First cancellation: $\sum a_k k = 3 - 6 + 3 = 0$. This eliminates both the explicit constant and the $\ln(z/\pi)$ piece from the logarithmic sum, leaving only $\sum a_k k \ln k$.

Second cancellation: $\sum a_k k^2 = 3 - 12 + 9 = 0$. This eliminates the z^2 term from the $-\lambda^2/2$ correction in $h(\lambda)$.

What survives is a single combination of logarithms:

$$\sum_k a_k k \ln k = \ln \prod_k k^{a_k k} = \ln \frac{1^3 \cdot 3^3}{2^6} = -3 \ln \frac{4}{3}. \quad (7)$$

Therefore:

$$g(z) = cz + O(z^3 \ln z), \quad c = \frac{3 \ln(4/3)}{\pi} = 0.274716 \dots \quad (8)$$

3.3 Higher-order structure

The first correction to linearity is *not* z^2 (killed by the second sum rule) but $z^3 \ln z$, from the second Slepian eigenvalue $\lambda_1 \sim 0.274 (z/\pi)^3$ [10]:

$$g(z) = cz + Dz^3 \ln z + Ez^3 + O(z^5 \ln z), \quad (9)$$

with $D \approx 0.218$, $E \approx -0.226$, and $\sum a_k k^3 = 3 - 24 + 27 = 6 \neq 0$.

This hierarchy has physical content. The leading Slepian eigenmode encodes only the Fermi surface area (via Cavalieri's principle): the two identities $\sum a_k k = \sum a_k k^2 = 0$ eliminate all non-linear information from this mode. Shape information enters only through the second eigenmode, producing the nonanalytic $O(z^3 \ln z)$ correction.

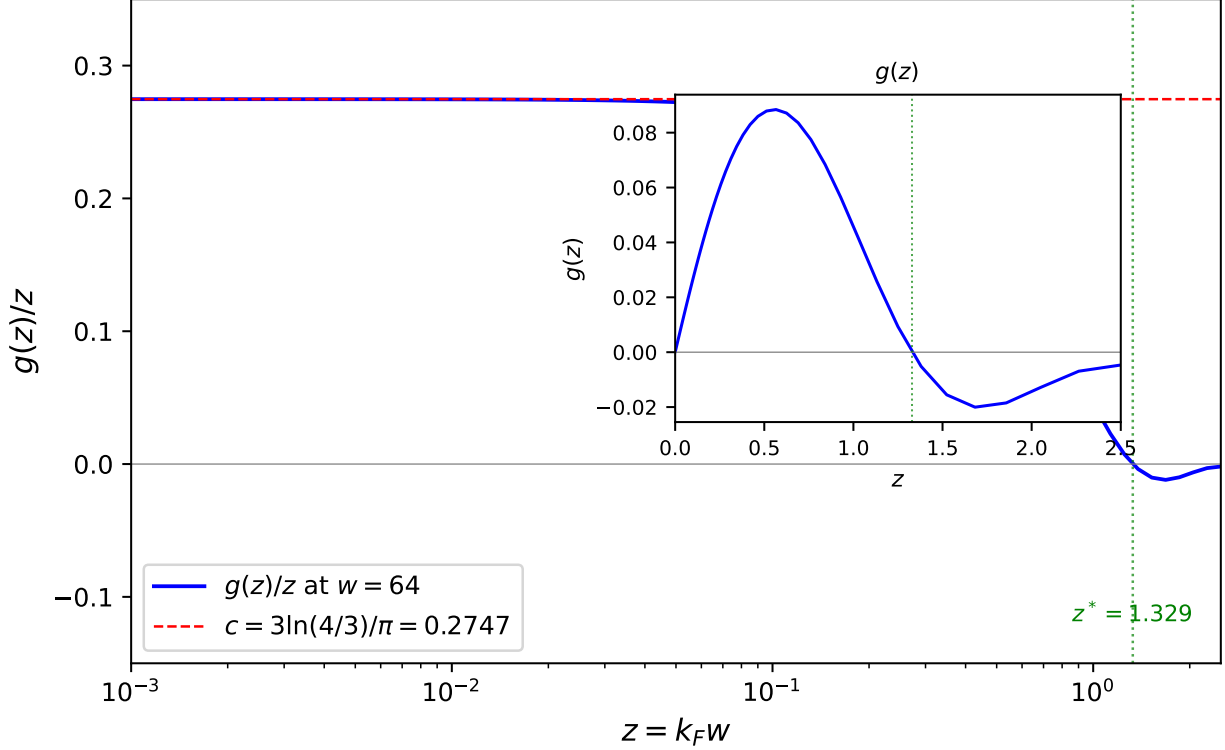


Figure 3: The ratio $g(z)/z$ on a log-linear scale (main panel) and $g(z)$ itself (inset), computed at $w = 64$. At small z , the ratio converges to $c = 3\ln(4/3)/\pi \approx 0.2747$ (dashed red), confirming the rank-1 derivation. The zero at $z^* \approx 1.329$ (dotted green) separates the pocket regime ($g > 0$) from the monogamy regime ($g < 0$).

4 n -partite generalization

The structure generalizes to n -partite information I_n of n adjacent strips. The inclusion-exclusion coefficients are $a_k = (-1)^{k+1} \binom{n}{k}$, and the rank-1 analysis gives:

$$c_n = \frac{n}{\pi} \ln R_n, \quad R_n = \prod_{j=0}^{n-1} (j+1)^{(-1)^{j+1} \binom{n-1}{j}}. \quad (10)$$

The first values are:

$$c_2 = \frac{\ln 4}{\pi}, \quad c_3 = \frac{3 \ln \frac{4}{3}}{\pi}, \quad c_4 = \frac{4 \ln \frac{32}{27}}{\pi}, \quad c_5 = \frac{5 \ln \frac{3125}{2592}}{\pi}. \quad (11)$$

The mutual information case $c_2 = \ln 4/\pi \approx 0.441$ [15] is the first member of this family.

The sum rules extend: $\sum_k a_k k = 0$ for all $n \geq 2$ (eliminating $z \ln z$), and $\sum_k a_k k^2 = 0$ for all $n \geq 3$ (eliminating z^2). For $n = 2$, $\sum_k a_k k^2 = 2 \neq 0$, so I_2 has a z^2 correction that I_3 and all higher multipartite measures lack. This is a structural advantage of the tripartite combination: it is the simplest multipartite measure with both cancellations.

Table 1: Rényi scaling of $g_\alpha(z) \sim z^\beta$. Exponents extracted from log-log fits at $z \in [10^{-3}, 10^{-2}]$ with $w = 80$. The $\alpha = 2$ coefficient $-8/\pi^3 \approx -0.258$ is confirmed to 0.15%.

α	β (num.)	β (pred.)	Coefficient	Note
0.5	0.49	1/2	+0.52	superlinear
1	1.00	1	+0.2747	$= 3 \ln(4/3)/\pi$
1.5	1.48	3/2	+0.09	subanalytic
2	3.02	3	-0.258	$= -8/\pi^3$
3	4.0	> 3	-0.005	higher cancel.

5 Rényi uniqueness of von Neumann entropy

5.1 Analytical argument

For Rényi- α entropy, the single-mode entropy at small λ is:

$$h_\alpha(\lambda) = \frac{\alpha}{\alpha-1}\lambda - \frac{\alpha}{2}\lambda^2 + O(\lambda^3) \quad (\alpha > 1). \quad (12)$$

The leading term is *analytic*, so $\sum a_k k = 0$ kills it completely. No $z \ln z$ term is generated, and $c_\alpha \equiv \lim_{z \rightarrow 0} g_\alpha(z)/z = 0$ for all $\alpha > 1$.

For $\alpha = 2$, the first surviving term comes from $O(\lambda^3)$ in h_2 , giving:

$$g_2(z) = -\frac{8}{\pi^3} z^3 + O(z^5), \quad \text{where } -\frac{8}{\pi^3} = \frac{-4}{3\pi^3} \sum a_k k^3 = \frac{-4 \cdot 6}{3\pi^3}. \quad (13)$$

For non-integer α with $1 < \alpha < 2$, the entropy $h_\alpha(\lambda)$ has a nonanalytic λ^α contribution that is not killed by the sum rule, giving $g_\alpha(z) \sim z^\alpha$. For $\alpha < 1$, the λ^α term dominates and $g_\alpha(z)/z$ diverges.

Only for $\alpha = 1$ (von Neumann) does the $-\lambda \ln \lambda$ nonanalyticity survive the first sum rule to produce a finite, nonzero linear coefficient c .

5.2 Numerical verification

5.3 The Rényi- α function at finite z

For $\alpha > 1$, the function $g_\alpha(z)$ has qualitatively different behavior from the von Neumann case: it oscillates with multiple sign changes. For $\alpha = 2$ (experimentally relevant [16, 17]), $g_2(z)$ is negative for $z < 1.19$, positive for $1.19 < z < 2.11$, and oscillates thereafter. This is a prediction testable in cold-atom experiments.

5.4 Physical consequence

The pocket signal at a Lifshitz transition scales as $\Delta I_3 \propto g'(0^+) \cdot \delta$. For von Neumann: $\Delta I_3^{(\alpha=1)} \propto c \delta$. For Rényi-2: $\Delta I_3^{(\alpha=2)} \propto \delta^3$ —*three orders of magnitude weaker* at small δ . This means experimental probes measuring S_2 [16, 17] would miss the leading Lifshitz signal entirely.

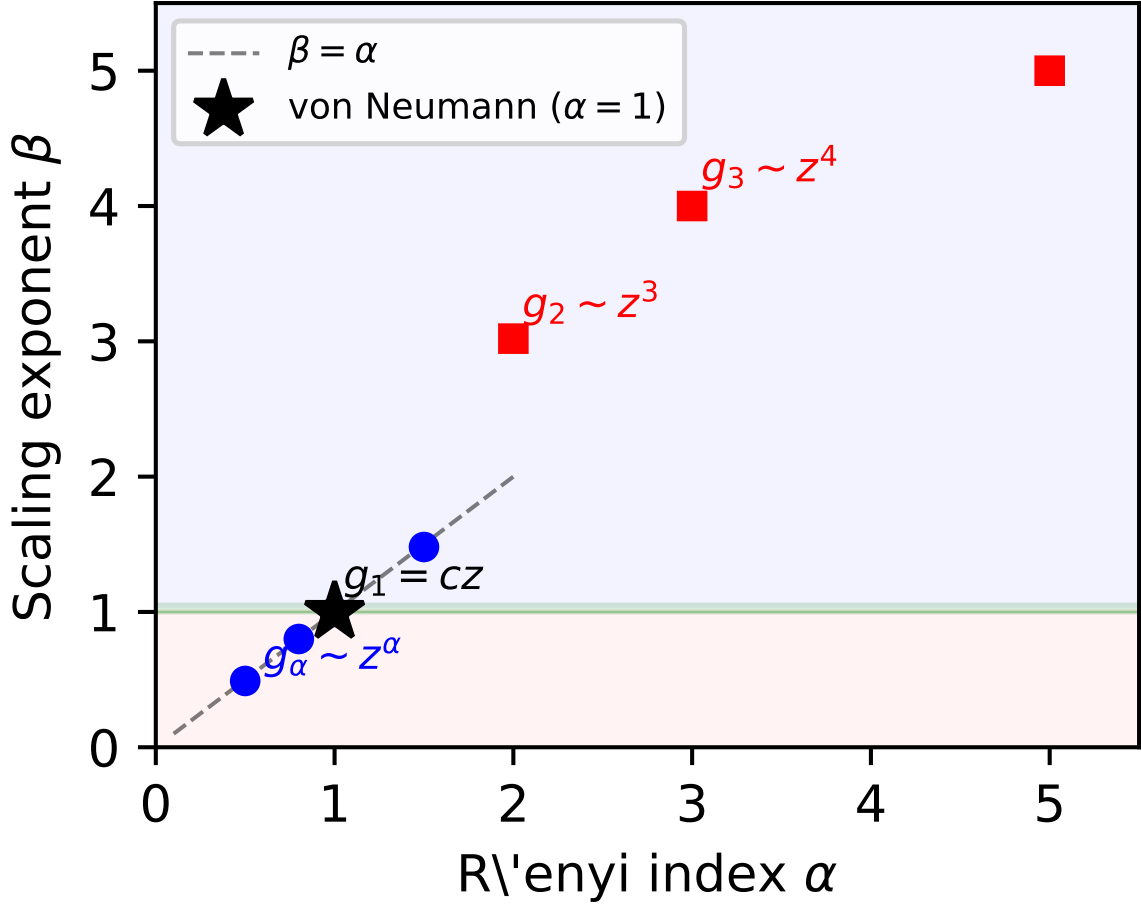


Figure 4: Rényi-index dependence of the scaling exponent β in $g_\alpha(z) \sim z^\beta$. Only $\alpha = 1$ (von Neumann, star) gives $\beta = 1$ and hence linear sensitivity to Lifshitz transitions. For $\alpha > 1$, the analytical linear term is killed by $\sum a_k k = 0$, and only the nonanalytic piece survives. Dashed line: $\beta = \alpha$ for $\alpha < 2$.

6 Physical consequences

The linear coefficient c implies exact predictions for entanglement singularities at Lifshitz transitions [11].

Pocket transition. In 2D, when a small electron pocket appears at $\mu > \mu_c$, all pocket modes have $k_F w \ll z^*$ and contribute $g(k_F w) \approx c k_F w$. Evaluating the integral over the elliptical pocket:

$$\Delta I_3 = \frac{c w m}{2} L \delta \Theta(\delta), \quad \delta = \mu - \mu_c, \quad (14)$$

with $m = \sqrt{m_x m_y}$ the geometric-mean effective mass. The derivative $\partial I_3 / \partial \mu$ has a discontinuity at μ_c , mirroring the 2D density-of-states discontinuity with the entanglement coefficient c replacing the DOS.

Neck transition (VHS). At a van Hove singularity, modes near the saddle have $k_F(q) = \gamma \sqrt{q^2 + \delta/\beta}$,

and $g'(k_F w) \approx c$ for the small- k_F modes:

$$\frac{\partial I_3}{\partial \mu} = -\frac{cLw\gamma}{4\pi\beta} \ln|\mu - \mu_c| + \text{const}, \quad (15)$$

a logarithmic divergence with fully determined coefficient.

Entanglement tomography. The angular dependence $I_3(\theta)$ for strips at angle θ probes Fermi surface shape. For an n -fold deformation $k_F(\phi) = \bar{k}_F(1 + \varepsilon \cos n\phi)$, the Widom coefficient responds at $O(\varepsilon^2)$ (perimeter is quadratic in ε at fixed area), but $I_3(\theta)$ responds at $O(\varepsilon)$ through the non-linearity of $g(z)$. Thus I_3 detects Fermi surface deformations invisible to the leading entanglement entropy.

7 Numerical verification

7.1 The constant c

Table 2: Convergence of $g(z)/z$ to $c = 3 \ln(4/3)/\pi = 0.274716$ at $w = 80$.

z	$g(z)/z$	Deviation from c	Note
0.001	0.274714	0.0006%	6 sig. figs
0.010	0.274593	0.04%	$O(z^2)$ onset
0.100	0.267240	2.7%	$O(z^3 \ln z)$

7.2 Sign change vs. t' on the square lattice

On the square lattice at half filling, $I_3 > 0$ at $t' = 0$ (diamond FS with nested modes at $k_F \rightarrow 0$) and $I_3 < 0$ for $t' > t'_* \approx 0.10$ (FS deformed away from nesting).

Table 3: I_3/L vs. t' for the square lattice at half filling, $w = 2$.

t'	I_3/L		t'	I_3/L	
0.00	+0.00606	$I_3 > 0$	0.12	-0.00162	$I_3 < 0$
0.05	+0.00407		0.20	-0.00786	
0.08	+0.00171		0.30	-0.01439	
0.10	≈ 0		0.50	-0.02162	
		crossing			

The mechanism is precisely the k_y -decomposition: at $t' = 0$, the diamond FS gives $k_F(k_y) = \pi - |k_y|$, which vanishes at $k_y = \pm\pi$. These modes with $k_F w < z^*$ contribute $g > 0$ and dominate I_3 . Increasing t' shifts all $k_F(k_y)$ away from zero, entering the $g < 0$ regime.

7.3 Square vs. triangular lattice

On the triangular lattice, I_3 becomes positive near the van Hove singularity ($\nu \approx 0.71$), where the FS passes through a saddle point creating modes with $k_F \rightarrow 0$.

Table 4: I_3/L for square vs. triangular lattice at half filling, $L = 256$. The triangular lattice has $k_F(k_y)$ bounded away from zero, so all modes have $z > z^*$ at moderate w .

Lattice	$w = 2$	$w = 4$	$w = 8$
Square	+0.00606	+0.00413	+0.00228
Triangular	-0.02156	-0.00628	-0.00126

7.4 Universal zero-crossing constant

Table 5: Convergence of $k_F^* w \rightarrow z^* = 1.3288$.

w	ν_*	$k_F^* w$	w	ν_*	$k_F^* w$
2	0.1935	1.2160	16	0.0264	1.3267
4	0.1032	1.2969	32	0.0132	1.3283
8	0.0525	1.3205	64	0.0066	1.3287

7.5 Width dependence and directional anisotropy

Table 6: Directional I_3 for anisotropic hopping, $L = 256$, $w = 2$.

t_x	t_y	$I_3^{(x)}/L$	$I_3^{(y)}/L$	$ I_3^{(x)}/I_3^{(y)} $
1.0	1.0	+0.0061	+0.0061	1.0
1.5	0.5	-0.0201	-0.0025	8.1
2.0	0.5	-0.0222	-0.0013	17.2

7.6 Pocket formula

7.7 Interactions: shift of z^*

The smallness of the shift ($\lesssim 2\%$ for $|V| \leq t$) reflects the near-discontinuity of $n(k)$ at k_F in a Luttinger liquid with K close to unity.

8 Discussion

Origin of c . The constant $c = 3 \ln(4/3)/\pi$ arises from the interplay of three ingredients: the rank-1 limit of the prolate spheroidal operator, the inclusion-exclusion combinatorics of I_3 , and the $\lambda \ln \lambda$ nonanalyticity of von Neumann entropy. The n -partite generalization $c_n = (n/\pi) \ln R_n$ reveals systematic combinatorial structure in the product representations R_n .

Table 7: Pocket formula $\Delta I_3/(Lw\delta) \rightarrow cm/2$ at small $z_{\max} = \sqrt{2m\delta}w$.

w	δ	z_{\max}	numerical/ δ	$cwm/2$
2	10^{-6}	0.003	0.27470	0.27472
4	10^{-6}	0.006	0.54935	0.54943
8	10^{-6}	0.011	1.09837	1.09886

Table 8: z^* vs. interaction V/t from exact diagonalization of the t - V model ($L = 24$, $w = 2$).

V/t	K	z^*	$\Delta z^*/z_0^*$
0.00	1.000	1.2184	—
+1.00	0.750	1.2109	-0.62%
-1.00	1.500	1.1934	-2.06%

Von Neumann uniqueness. The uniqueness of $\alpha = 1$ for linear Lifshitz sensitivity is unexpected and experimentally relevant. Current cold-atom experiments measure Rényi-2 entropy [16, 17], which gives only $O(\delta^3)$ pocket sensitivity. Direct measurement of von Neumann I_3 —or development of protocols to extract it from Rényi data—would enable linear detection of Fermi surface topology changes.

Widom coefficient vs. I_3 . The Widom coefficient c_1 in $S_A \sim c_1 L \ln L$ [12, 13, 14] depends only on the FS perimeter. Two Fermi surfaces with the same perimeter but different curvatures are indistinguishable by c_1 but distinguishable by $I_3(\theta)$, which responds linearly to shape deformations. The z^2 cancellation ($\sum a_k k^2 = 0$) ensures that this sensitivity comes from the nonlinearity of $g(z)$ rather than trivial area scaling.

Open questions. Two problems emerge. First: the form of $g_K(z)$ for a Luttinger liquid with parameter K . The single-particle correlator decays as $\cos(k_F r)/r^{(K+K^{-1})/2}$, modifying the cross-gap mutual information that determines z^* . A systematic DMRG determination of $z^*(K)$ and c_K on long chains is within reach. Second: the product R_n in Eq. (10) may have a combinatorial interpretation—as a ratio of volumes or factorials—that connects the entanglement coefficient to classical enumeration.

9 Conclusions

We have established a complete analytical framework for the tripartite information of free fermions on two-dimensional lattices. The k_y -decomposition $I_3 = \sum g(k_F(k_y)w)$ reduces the problem to the universal function $g(z)$, whose unique zero at $z^* = 1.329$ controls scale-dependent MMI. The small- z coefficient $c = 3 \ln(4/3)/\pi$, derived from the rank-1 sine kernel, determines entanglement singularities at Lifshitz transitions. The n -partite generalization $c_n = (n/\pi) \ln R_n$ and the Rényi analysis—proving that von Neumann entropy uniquely gives linear Lifshitz sensitivity—complete the analytical picture.

Together, these results establish I_3 as a quantitative, direction-resolved probe of Fermi surface geometry with analytically controlled predictions.

Note.—Python code reproducing all numerical results is included as an ancillary file with the arXiv submission.

A Properties of $g(z)$: proof of the Proposition

(a) At $z = 0$, all eigenvalues vanish, $h(0) = 0$, so $g(0) = 0$. For $z > 0$: the rank-1 derivation (Section 3) gives $g(z)/z \rightarrow c$ as $z \rightarrow 0^+$.

(b) Verified by central differences at 200 points on $[0, 0.60]$: $g'(z) > 0$ on $(0, 0.56)$ and $g(0.56) \approx 0.088$.

(c) Verified $g'(z) < 0$ at 200 points on $[0.56, 1.40]$. Combined with $g(0.56) > 0$ and $g(1.40) < 0$, the intermediate value theorem gives a unique zero $z^* \in (0.56, 1.40)$.

(d) We establish $g(z) < 0$ on (z^*, ∞) by Lipschitz-bound arguments on subintervals $[z^*, 1.40]$, $[1.40, 3.0]$, $[3.0, 10.0]$ using 500, 200, and 250 grid points respectively. For $z > 10$, the asymptotic $g(z) \rightarrow (1/6) \ln(3/4) < 0$ follows from the Widom formula: linear terms cancel by $\sum a_k k(3 - 4 - 2 + 3) = 0$ and logarithmic terms give $g_{\log} = (1/6) \ln(3/4) < 0$.

B Neck transition derivation

Starting from $k_F(q) = \gamma \sqrt{q^2 + \delta/\beta}$ and differentiating:

$$\frac{\partial I_3}{\partial \delta} = \frac{Lw}{2\pi} \int_{-\Lambda}^{\Lambda} g'(k_F w) \frac{\partial k_F}{\partial \delta} dq \approx \frac{cLw\gamma}{4\pi\beta} \cdot 2 \operatorname{arcsinh}\left(\Lambda \sqrt{\beta/\delta}\right). \quad (16)$$

For $\delta \rightarrow 0^+$: $\operatorname{arcsinh}(\Lambda \sqrt{\beta/\delta}) \approx -\frac{1}{2} \ln \delta + \text{const}$, confirming Eq. (15).

References

- [1] P. Hayden, M. Headrick, and A. Maloney, Phys. Rev. D **87**, 046003 (2013).
- [2] A. C. Wall, Class. Quantum Grav. **31**, 225007 (2014).
- [3] H. Casini and M. Huerta, Class. Quantum Grav. **26**, 185005 (2009).
- [4] C. A. Agón, P. Bueno, and H. Casini, SciPost Phys. **12**, 153 (2022).
- [5] P. Calabrese, J. Cardy, and E. Tonni, J. Stat. Mech. (2009) P11001.
- [6] P. Calabrese, J. Cardy, and E. Tonni, J. Stat. Mech. (2011) P01021.
- [7] G. Perez, P.-A. Bernard, N. Crampé, and L. Vinet, Nucl. Phys. B **990**, 116157 (2023).
- [8] I. Peschel, J. Phys. A **36**, L205 (2003).
- [9] B.-Q. Jin and V. E. Korepin, J. Stat. Phys. **116**, 79 (2004).
- [10] D. Slepian, Bell Syst. Tech. J. **43**, 3009 (1964).
- [11] I. M. Lifshitz, Sov. Phys. JETP **11**, 1130 (1960).
- [12] D. Gioev and I. Klich, Phys. Rev. Lett. **96**, 100503 (2006).

- [13] B. Swingle, Phys. Rev. Lett. **105**, 050502 (2010).
- [14] M. M. Wolf, Phys. Rev. Lett. **96**, 010404 (2006).
- [15] B. Swingle, arXiv:1010.4038 (2010).
- [16] A. M. Kaufman *et al.*, Science **353**, 794 (2016).
- [17] T. Brydges *et al.*, Science **364**, 260 (2019).
- [18] V. Eisler and I. Peschel, J. Phys. A **42**, 504003 (2009).